Journal of Magnetism and Magnetic Materials 429 (2017) 69–73

Contents lists available at ScienceDirect

Journal of Magnetism and Magnetic Materials

journal homepage: www.elsevier.com/locate/jmmm

Annealing temperature dependent non-monotonic d^0 ferromagnetism in pristine In_2O_3 nanoparticles

Haiming Cao, Pengfei Xing*, Dongsheng Yao, Ping Wu

Department of Applied Physics, Institute of Advanced Materials Physics, Tianjin Key Laboratory of Low Dimensional Materials Physics and Preparing Technology, Faculty of Science, Tianjin University, Tianjin 300072, PR China

ARTICLE INFO

Keywords:
d^0 ferromagnetism
Indium oxide
Nanoparticle
Air-annealing
Oxygen vacancy
Sol-gel

ABSTRACT

Cubic bixbyite In_2O_3 nanoparticles with room temperature d^0 ferromagnetism were prepared by sol-gel method with the air annealing temperature ranging from 500 to 900 °C. X-ray diffraction, X-ray photoelectron spectroscopy, Raman-scattering and photoluminescence were carried out to demonstrate the presence of oxygen vacancies. The lattice constant, the atomic ratio of crystal O and In, the Raman peak at 369 cm^{-1}, the PL emission peak at 396 nm and the saturation magnetization of d^0 ferromagnetism all had a consistent non-monotonic change with the increasing annealing temperature. With further considering the relation between the grain size and the distribution of oxygen vacancies, we think that d^0 ferromagnetism in our samples is directly related with the singly charged oxygen vacancies at the surface of In_2O_3 nanoparticles.

1. Introduction

Since room temperature ferromagnetism (RTFM) in Mn-doped ZnO was predicated by Dietl et al. [1] in 2000, diluted magnetic oxide semiconductors have attracted much attention due to the potential to control spin and charge simultaneously in spintronic devices. A great many of experimental and theoretical works have been carried out on transition-metal elements doped oxides, such as ZnO, TiO_2, SnO_2 and In_2O_3, etc. But the origin of the ferromagnetism is still in dispute for the possibility that the ferromagnetism may be from the ferromagnetic clusters, precipitations or other secondary phases is hard to be ruled out. In 2004, d^0 ferromagnetism was firstly reported in undoped HfO_2 thin films, which opens a new way for further exploring the mechanism of ferromagnetism in nonmagnetic oxides [4]. d^0 ferromagnetism has also been found in CeO_2, Al_2O_3, ZnO, SnO_2 and TiO_2 in low dimensional forms, such as nanoparticles [5–9], nanowires [10], nanorods [11] and thin films [12], etc. However, despite the intense research, the origin of the d^0 ferromagnetism still remains a controversial unresolved problem.

As a widely applied material in transparent conducting films, solar cells, flat-panel displays and gas sensing field [2,13], indium oxide is also considered as a base material for magnetic semiconductors, and d^0 ferromagnetism in pure In_2O_3 system has been intensively investigated in the recent years. Experimentally, Sun et al. reported that d^0 ferromagnetism in In_2O_3 thin films stemmed from the single ionized oxygen and indium vacancies [2,3], while Sundaresan et al. attributed the d^0 ferromagnetism in In_2O_3 nanoparticles to oxygen vacancies (Vo) at the surface of nanoparticles [5]. However, Qaseem et al. attributed the size induced d^0 ferromagnetism in pristine indium oxide nanoparticles to the defect density and size confinement effect [7]. Theoretically, Xiao et al. claimed that the interaction between In s-p hybridization orbits was responsible for d^0 ferromagnetism in oxygen-depleted In_2O_3 (001) surfaces [14], while Wang et al. argued that the FM in In_2O_3 quantum dots was introduced by surface oxygen dangling bonds and Indium vacancies [15]. Although the reported d^0 ferromagnetism in In_2O_3 system mentioned above is mainly attributed to the existence of native defects, such as oxygen vacancy, cation vacancy and other complex structures of defects, further researches are still needed to define when a specific kind of defect plays a role and how the coupling happens.

Comparing with the bulk and film system, there are more surfaces in nanoparticles where oxygen vacancies tend to gather. So it is worth noting that the nanoparticle with high surface-to-volume ratio is an ideal system for studying the role that oxygen vacancies play in mediating d^0 ferromagnetism. In this paper, we report d^0 ferromagnetism in In_2O_3 nanoparticles, which was prepared by sol-gel method with the air annealing temperature ranging from 500 to 900 °C. The consistent results of the structural, optical and magnetic properties indicate that singly charged oxygen vacancies (V_O^+) at the surface of the nanoparticles play an important role in mediating d^0 ferromagnetism in pure In_2O_3 system.

* Corresponding author.
E-mail address: pfxing@tju.edu.cn (P. Xing).

http://dx.doi.org/10.1016/j.jmmm.2017.01.015
Received 31 October 2016; Received in revised form 26 December 2016; Accepted 5 January 2017
Available online 06 January 2017

2. Experimental details

Indium oxide nanoparticles were synthesized by sol-gel method. Indium oxide precursor was prepared by dissolving stoichiometric amounts of Indium (III) nitrate hydrate ($In(NO_3)_3{\cdot}4H_2O$, 99.9%), citric acid (AR) and ethylene glycol (AR) in ethanol (GR). The mixture was firstly stirred at 90 °C for 6 h to form a wet white gel, which was then transferred into a drying oven at 120 °C for 8 h to evaporate excess ethanol and swelled into a foamed dark brown gel. After that, the gel was calcined at 350 °C for 12 h to carry out the combustion reaction, and ground into light yellow as-grown powders. Finally, the as-grown powders were annealed at certain temperatures of 500, 600, 700, 800 and 900 °C, respectively, for 70 min in air to get a series of samples, which were referred as A1-A5, accordingly. Besides, annealing in Ar ambient was also carried out on A1 and A3 at 500 and 700 °C, respectively, for 70 min. The corresponding samples were labeled as AA1 and AA3.

The structure and phase identification were characterized by X-ray diffraction (XRD) using a diffractometer (Rigaku D/MAX-2500) with Cu Kα radiation. The morphology and grain size were examined by a scanning electron microscope (SEM, Hitachi S4800). The valence and the effective concentration of elements were characterized with an X-ray photoelectron spectroscopy (XPS, PHI1600). The defect states were studied by using a Raman-scattering spectrometer (RENISHAW inVia) with a 532 nm laser line at room temperature. Optical properties were analyzed by a photoluminescence (PL) spectrometer (PL, Fluorolog3-21 Fluorescence Spectrometer) at room temperature. Magnetization measurements were carried out with a magnetic properties measurement system (MPMS, Quantum Design).

3. Results and discussion

Fig. 1(a) shows the XRD patterns of A1, A2, A3, A4 and A5, which indicates that all peaks are indexed well to the standard cubic bixbyite In_2O_3 (PDF, 71–2194, space group *Ia-3* (206)). No peaks of impurities or other indium-related secondary phases are observed within the detection limit. The peak intensity is enhanced with the increase of annealing temperature, which shows the crystallization quality is improved by the higher annealing temperature. Fig. 1(b) shows the relative changes in the grain size and lattice constant for A1-A5. The average grain sizes of the samples were calculated by using the Debye-Scherrer equation. As we can see, the grain size increases monotonously from 16.8 to 43.5 nm with the annealing temperature increasing from 500 to 900 °C, which can be attributed to that higher annealing temperatures can supply more energy for recrystallization. However, the lattice constant changes non-monotonically with the increase of annealing temperature. As the annealing temperature increases from 500 to 700 °C, the lattice constant increases rapidly from 10.1190 to 10.1226 Å. This is mainly caused by the lattice expansion and the reduction of the oxygen vacancies, for Vo tend to appear in samples prepared at lower temperatures [13]. When the annealing temperature is further increased to 900 °C, a slightly decrease in the lattice constant to 10.1222 Å is detected, which can be mainly ascribed to that the annealing temperature is too high to hold the lattice oxygen during the unit cell growth [16]. New oxygen vacancies appear, and the lattice constant decreases. In order to observe the morphology of the samples more directly, the SEM pattern of A1 is depicted in Fig. 1(c). From the figure, we can see that no impurities or other clusters are observed in the vision. The outline of the particles is mostly cube-like, which matches well with the cubic structure of In_2O_3. It can also be seen that the mean size of the nanoparticles is approximately 20 nm, which is consistent with the XRD results.

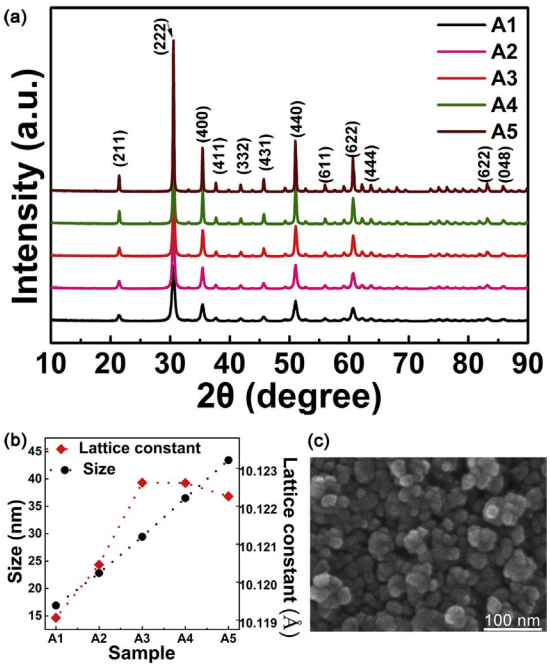

Fig. 1. (a) XRD patterns of A1, A2, A3, A4 and A5. (b) The mean grain size (circle) and lattice constant (diamond) of A1-A5. (c) The SEM pattern of A1.

Fig. 2(a) shows the XPS spectrum of A1 depicting a range scan from 0 to 1100 eV. Similar spectra are also obtained for other samples which are not shown here. Peaks such as O 1s, In 3s, In 3p, In 3d, In 4s, In 4p, In 4d and C 1s are detected. No other impurity peaks are detected in the detection limit, indicating that all our samples are clean without any contamination. Fig. 2(b) shows In $3d_{3/2}$ and In $3d_{5/2}$ peaks of A1,

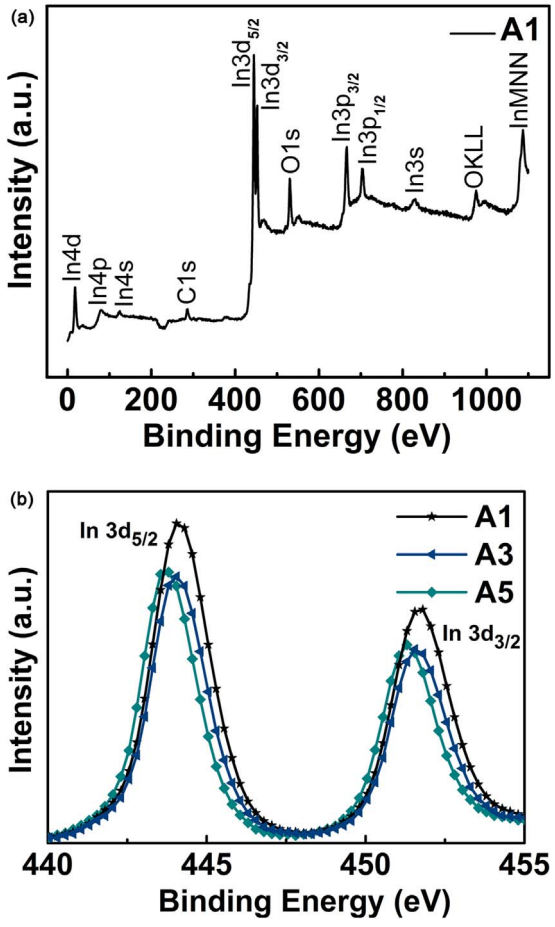

Fig. 2. (a) XPS full spectrum of A1 depicting a range scan from 0 to 1100 eV. Similar spectra were also obtained for A3 and A5. (b) In 3d XPS spectra of A1 (star), A3 (triangle) and A5 (diamond).